Clinical Epigenetics

RESEARCH

Open Access

Effects of stressful life-events on DNA methylation in panic disorder and major depressive disorder

Darina Czamara[1*], Alexa Neufang[2], Roman Dieterle[2], Stella Iurato[1], Janine Arloth[1], Jade Martins[1], Marcus Ising[1], Elisabeth E. Binder[1,3] and Angelika Erhardt[1,4]

Abstract

Background: Panic disorder (PD) is characterized by recurrent panic attacks and higher affection of women as compared to men. The lifetime prevalence of PD is about 2–3% in the general population leading to tremendous distress and disability. Etiologically, genetic and environmental factors, such as stress, contribute to the onset and relapse of PD. In the present study, we investigated epigenome-wide DNA methylation (DNAm) in respond to a cumulative, stress-weighted life events score (wLE) in patients with PD and its boundary to major depressive disorder (MDD), frequently co-occurring with symptoms of PD.

Methods: DNAm was assessed by the Illumina HumanMethylation450 BeadChip. In a meta-analytic approach, epigenome-wide DNAm changes in association with wLE were first analyzed in two PD cohorts (with a total sample size of 183 PD patients and 85 healthy controls) and lastly in 102 patients with MDD to identify possible overlapping and opposing effects of wLE on DNAm. Additionally, analysis of differentially methylated regions (DMRs) was conducted to identify regional clusters of association.

Results: Two CpG-sites presented with *p*-values below 1×10^{-05} in PD: cg09738429 ($p = 6.40 \times 10^{-06}$, located in an intergenic shore region in next proximity of *PYROXD1*) and cg03341655 ($p = 8.14 \times 10^{-06}$, located in the exonic region of *GFOD2*). The association of DNAm at cg03341655 and wLE could be replicated in the independent MDD case sample indicating a diagnosis independent effect. Genes mapping to the top hits were significantly upregulated in brain and top hits have been implicated in the metabolic system. Additionally, two significant DMRs were identified for PD only on chromosome 10 and 18, including CpG-sites which have been reported to be associated with anxiety and other psychiatric phenotypes.

Conclusion: This first DNAm analysis in PD reveals first evidence of small but significant DNAm changes in PD in association with cumulative stress-weighted life events. Most of the top associated CpG-sites are located in genes implicated in metabolic processes supporting the hypothesis that environmental stress contributes to health damaging changes by affecting a broad spectrum of systems in the body.

Keywords: Panic disorder, Major depressive disorder, Stressful life events, EWAS

Background

Panic disorder (PD) is characterized by recurrent, unexpected panic attacks which are associated with extreme anxiety and fear levels and a wide range of further psychological and somatic symptoms, such as fear of dying,

*Correspondence: darina@psych.mpg.de
[1] Translational Department, Max Planck Institute for Psychiatry, Kraepelinstrasse 2+10, 80804 Munich, Germany
Full list of author information is available at the end of the article

feeling of being out of control, heart racing palpitations, difficulties to breathe and tightness in the chest [1]. Affected individuals often experience concerns about future panic attacks, which leads to phobic avoidance and long-term negative changes in daily life functions as well as psychological distress [2]. As such, PD is often associated with agoraphobia, characterized by panic attacks in situations where patients feel trapped or are unable to escape [3]. The lifetime prevalence of PD is about 2–3% in the general population and women are affected as twice as high as men [4, 5]. The comorbidity with further psychiatric conditions is high, specifically with anxiety disorders or depression [6]. Despite the availability of treatment options for PD, such as medication and psychotherapy, more than one third of patients respond only partially, continuing to have sub-threshold panic symptoms, and a considerable proportion of affected individuals relapse later in life [7].

The etiology of PD is considered to be complex involving genetic and environmental factors and their interaction [8]. Approximately 30–40% of disease etiology are assigned to genetics, consisting of common and rare variations across the genome and suggested higher proportion of genetic contribution in those reporting familial aggregation and early disease onset [9]. Following this, environmental influences, and more specifically, mostly unique individual experiences, are etiologically highly relevant on shaping biological processes which lead to the risk for clinical symptomatology [10]. According to the latter twin study, the proportion of variance in liability for PD attributable to environment ranges to 0.7 (0.59 individual environment, 0.11 shared environment). As such, stress is one of the candidate environmental triggers associated with higher risk for PD and anxiety disorders in general [11]. Although not many studies are available on specific stressors predisposing to PD, some evidence shows that childhood adversities, more recent separation and loss events as well as long-lasting stressful conditions, are associated with panic pathology with odds ratios ranging between 1.39 and 2.52 indicating substantial effects [12].

Environmental influences can induce long-lasting alterations in neurobiological systems, e.g., mediated by epigenetic mechanisms [13]. Epigenetics describes gene regulatory processes without changing the original DNA sequence. These modifications can be time-stable, heritable and responsive to environmental influences [14]. One of the epigenetic mechanisms increasingly studied in psychiatric research is DNA methylation (DNAm), which occurs on cytosines through addition of a methyl-group [15]. In consequence, this process modulates gene expression by regulating the accessibility of transcription factors to their binding sites.

The epigenetic research in PD is only at an early stage [16]. Most studies investigated DNAm between PD patients and controls on categorical level focusing on candidate genes from the monoamine systems, but first epigenome-wide association studies (EWAS) have been completed with interesting novel candidate findings, e.g., related to the immune and endogene stress system [17, 18]. Few studies are available regarding the influence of life events (LE) on DNAm in PD with first interesting results. One study investigated recent negative LE and DNAm in the gene *Glutamate Decorboxylase* (*GAD1*) involved in GABA synthesis and showed overall lower DNAm levels, specifically for female PD patients [19]. Similar results have been reported for the *Monoamine Oxidase A* gene (*MAOA*) [20]. Finally, one study investigating a novel candidate gene for PD, *TMEM132D*, derived from a genome-wide association study (GWAS) [21], showed a positive correlation of DNAm with positive LE [22]. However, no EWAS on LE and PD has been available yet.

PD often co-occurs with major depression (MDD), the lifetime comorbidity rates are estimated at 50–80% [23, 24]. PD and MDD are characterized as stress-related disorders as stressful life events are important contributing factors to the etiology and clinical course in both disorders. Generally, it is unclear which molecular pathways induced by external stress are common between PD and MDD and which might be specific for to the phenotypic difference. Therefore, in addition to the first evidence on shared and distinct genetic basis between PD and MDD from cross-disorder GWAS data [25], stress-induced DNAm changes might be the missing link to explain common and disorder-specific biological patterns. To date, one study by Zannas et al. in MDD analyzed EWAS data and stress on age prediction and epigenetic clocks. The results showed that cumulative life stress was linked to accelerated epigenetic age and that this effect could be driven by glucocorticoid induced DNAm [26].

In the present study, we investigated the influence of LE on epigenome-wide DNAm in two PD cohorts (183 patients with PD in total) as well as the interaction between PD status and LE. As the stressfulness of LE may vary between subjects, we additionally evaluated the perceived burden related to the reported LE. Given the high comorbidity of PD with MDD, we additionally conducted the same analysis in a case sample of MDD including 102 patients in order to confer disease-specific and common DNAm changes in response to LE.

Results

An overview of all performed analyses is given in Additional file 1: Fig. S1.

EWAS on weighted stressful life events in panic disorder

First, we assessed associations of weighted stressful life events (wLE), weighted positive (wposLE) and weighted negative LE (wnegLE) with DNA methylation (DNAm) levels in the PD discovery (PDI) and replication (PDII) case samples (see Table 1) on an epigenome-wide scale. Afterward, we meta-analyzed the results from both cohorts. Manhattan- and QQ-plots for the individual EWAS in PDI and PDII as well as for the meta-analysis are depicted in Additional files 2–4: Figs. S2–S4.

While no result was significant at FDR of 5%, two CpG-sites represented with *p*-values below 1.0×10^{-05} (see Table 2 and Additional file 4: Fig. S4) in the meta-analysis of wLE: cg03341655 (see Fig. 1A), an exonic CpG in *Glucose-fructose oxidoreductase domain containing 2* (*GFOD2)* gene on chromosome 16, and cg09738429 (see Fig. 1B), located in an intergenic region on chromosome 12 between the *Solute carrier organic anion transporter family, member 1A2 (SLCO1A2,* 102 kb downstream) and in the next proximity of *Pyridine nucleotide-disulphide oxidoreductase domain 1* (*PYROXD1*, 87 bp upstream). For both CpG-sites in discovery as well as in the replication cohort, PD cases presented with higher levels of wLE and lower DNAm levels. Neither the top hit of the EWAS on PD nor the studied candidate genes in Iurato et al. [18] were associated with wLE.

The weighted LE score included positive as well as negative events but was mainly correlated with weighted negative LE (wnegLE, discovery sample PDI: Spearman's $r = 0.90$, $p = 1.88 \times 10^{-20}$, replication sample PDII: Spearman's $r = 0.88$, $p = 1.26 \times 10^{-26}$) and to a far lower extent with weighted positive LE (wposLE, PDI: Spearman's $r = 0.24$, $p = 0.083$, PDII: Spearman's $r = 0.29$, $p = 0.01$). Weighted positive and weighted negative LE were not correlated with each other (PDI: Spearman's $r = 0.05$, $p = 0.69$, PDII: Spearman's $r = 0.06$, $p = 0.58$). We therefore repeated the analysis on wposLE (see Additional files 5–7: Figs. S5–S7) and wnegLE separately (see Additional files 8–10: Figs. S8–S10). Again, no CpG-sites were significant at FDR of 5%. Seven CpG-sites presented with *p*-values below 1.0×10^{-05} in the meta-analysis of wposLE, 8 CpGs in the meta-analysis of wnegLE, no CpGs overlapped (see Additional file 11: Tables S1 and S2). Furthermore, no CpGs were significantly differentially associated with

Table 1 Demographics of included samples

	PD discovery (PDI)	PD replication (PDII)	MDD cases	*p*-value Chi-Square*	*p*-value ANOVA*
n	109	159	102		
Cases (%)	87 (79.81%)	96 (60.38%)	102 (100%)	< 0.01	NA
Controls (%)	22 (20.19%)	63 (39.62%)	NA	< 0.01	NA
Male (%)	44 (40.37%)	54 (33.96%)	64 (62.75%)	< 0.01	NA
Female (%)	65 (59.63%)	105 (66.04%)	38 (37.25%)	< 0.01	NA
Mean age (SD)	47.65 (9.65)	38.23 (10.27)	47.76 (13.63)	NA	< 0.01
Mean log wLE (SD) in cases	4.16 (0.61)	4.21 (0.67)	4.26 (0.61)	NA	0.59

* *p*-value for differences in means of quantitative variables are based on ANOVA, *p*-values for differences in proportions of categorical variables are based on Chi-Square-Test

wLE: weighted life events

Table 2 Top hits of meta-analysis of wLE in PD discovery (PDI) and replication sample (PDII)

CpG	beta_meta	p_meta	p_meta_corrected	beta_PDI	p_PDI	beta_PDII	p_PDII
cg09738429	− 0.2656	6.40×10^{-06}	1.00	− 0.2798	2.36×10^{-04}	− 0.2382	2.05×10^{-02}
cg03341655	− 0.1077	8.14×10^{-06}	1.00	− 0.0686	1.67×10^{-01}	− 0.1201	3.98×10^{-05}

beta_meta: effect-size estimate in meta-analysis

p_meta: nominal *p*-value from meta-analysis

p_meta_corrected: Benjamini–Hochberg FDR-corrected *p*-value from meta-analysis

beta_PDI: effect-size estimate in PDI

p_PDI: nominal *p*-value in PDI

beta_PDII: effect-size estimate in PDII

p_PDII: nominal *p*-value in PDII

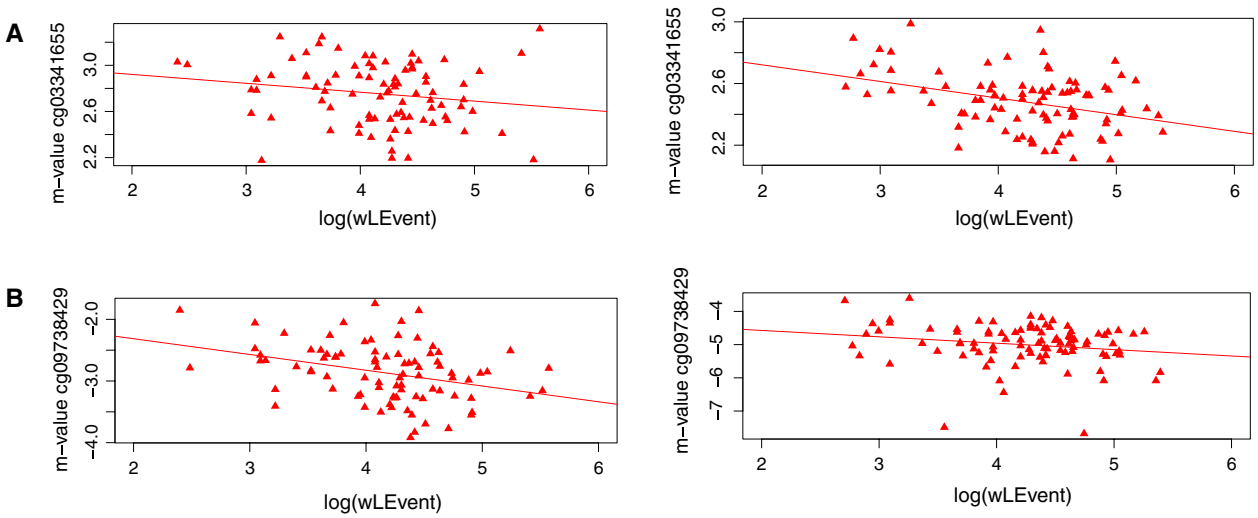

Fig. 1 Scatterplots for top hits of meta-analysis on EWAS in PD discovery and PD replication sample. Scatter plot of *M*-value of cg03341655 (*y*-axis) and log(wLE) (*x*-axis) in PD discovery (left) and replication sample (right) (**A**). Scatter plot of *M*-value of cg09738429 (*y*-axis) and log(wLE) (*x*-axis) in PD discovery **(**left) and replication sample (right) (**B**)

wposLE and wnegLE, i.e., showing different effect directions between positive and negative LE, with *p*-values below 1.0×10^{-03}.

Pathway enrichment analysis of top hits

Next, we performed a pathway enrichment analysis based on all genes mapping to CpG-sites associated with wLE with *p*-values < 0.01 in the meta-analysis (1995 CpG-sites mapping to 1742 unique genes). We used genes mapping to all CpG-sites included in the meta-analysis as background (424,763 CpG-sites mapping to unique 19,563 genes).

Genes mapping to the top hits were specifically expressed in brain ($p = 7.73 \times 10^{-05}$), followed by blood vessel, breast and Fallopian tube (see Additional file 11: Table S3). The enrichment for brain was mainly driven by CpG-sites which were higher methylated with higher wLE scores (872 hypermethylated CpGs-sites mapping to 787 unique genes, see Additional file 11: Table S4). CpG-sites which were lower methylated with higher wLE scores (1123 hypomethylated CpGs mapping to 1024 unique genes) did not show any tissue-specific enrichments (see Additional file 11: Table S5). A similar pattern arose for enrichment for GO biological processes: genes matching to top hits, regardless of direction, were significantly enriched for 247 GO biological processed terms including embryo ($p = 1.24 \times 10^{-14}$) and neuron development ($p = 7.96 \times 10^{-09}$, see Additional file 11: Table S6). These enrichments were again mainly driven by hypermethylated CpG-sites (enriched for 137 terms, see Additional file 11: Table S7; hypomethylated CpG-sites were enriched for only 52 terms, see Additional file 11: Table S8).

DMR of weighted stressful life events

Analysis on DMRs of wLE revealed two significant regions at FDR 5% (see Table 3): DMR I located in an intergenic region on chromosome 10: 10,1282,726–101,282,884 between *GOT1* (92 kb downstream) and *DQ372722* (3 kb upstream) and consisting of 4 CpG-sites (cg01987516, cg07044859, cg17888390 and cg23904955) where individuals with a higher score of wLE presented with higher DNAm levels (see Fig. 2A). Direction of effects was opposite for DMR II located in an intergenic region on chromosome 18: 72,837,531–72,837,701 between *ZNF407* (60 kb downstream) and *ZADH2* (72 kb upstream), consisting of 4 CpG-sites (cg04756515, cg14395744, cg18709881 and cg21894287, see Fig. 2B).

Interaction of PD versus control status on wLE

Next, we investigated interaction effects of case–control status and wLE on DNAm, i.e., if the association of wLE on DNAm differed between PD cases and controls (see Additional files 12–14: Figs. S11–S13). We observed no significant interaction for single CpGs or for DMRs in the meta-analysis passing multiple testing correction. Seven CpGs presented with interaction *p*-values below 1.0×10^{-05} (see Additional file 11: Table S9). The strongest interaction was observed for *cg20941758*, an intronic CpG-site in *NKAIN1* on chromosome 1 (p_interaction_meta = 1.52×10^{-06}, see Additional file 15: Fig. S14). While PD cases presented with higher DNAm levels with

Table 3 Top hits of DMR-analysis of wLE in PD discovery (PDI) and replication sample (PDII)

CpGs included in DMR	Position (hg19)	beta_PDI	p_PDI	beta_PDII	beta_PDII	p_DMR	p_DMR_corrected
cg01987516, cg07044859, cg17888390, cg23904955	chr10: 10,1282,726–101,282,884	1.4077	1.14×10^{-02}	1.0837	4.91×10^{-03}	2.11×10^{-11}	5.60×10^{-08}
cg04756515, cg14395744, cg18709881, cg21894287	chr18: 72,837,531–72,837,701	−1.008	5.49×10^{-02}	−0.7770	1.18×10^{-02}	2.03×10^{-08}	5.06×10^{-05}

beta_PDI: effect-size estimate in PDI when taking the mean methylation M-values across all CpGs included in the DMR

p_PDI: nominal *p*-value in PDI when taking the mean methylation M-values across all CpGs included in the DMR

beta_PDII: effect-size estimate in PDII when taking the mean methylation M-values across all CpGs included in the DMR

p_PDII: nominal *p*-value in PDII when taking the mean methylation M-values across all CpGs included in the DMR

p_DMR: nominal *p*-value from DMR-analysis in comb-p on the meta-analysis of PDI and PDII

p_DMR_corrected: *p*-value from DMR-analysis in comb-p on the meta-analysis of PDI and PDII corrected for multiple testing across all tested regions

The DMR analysis was performed in comb-p. The effect sizes in PDI and PDII using the mean *M*-values are just displayed for illustration. Comb-p uses the meta-analysis *p*-values of the single CpGs directly

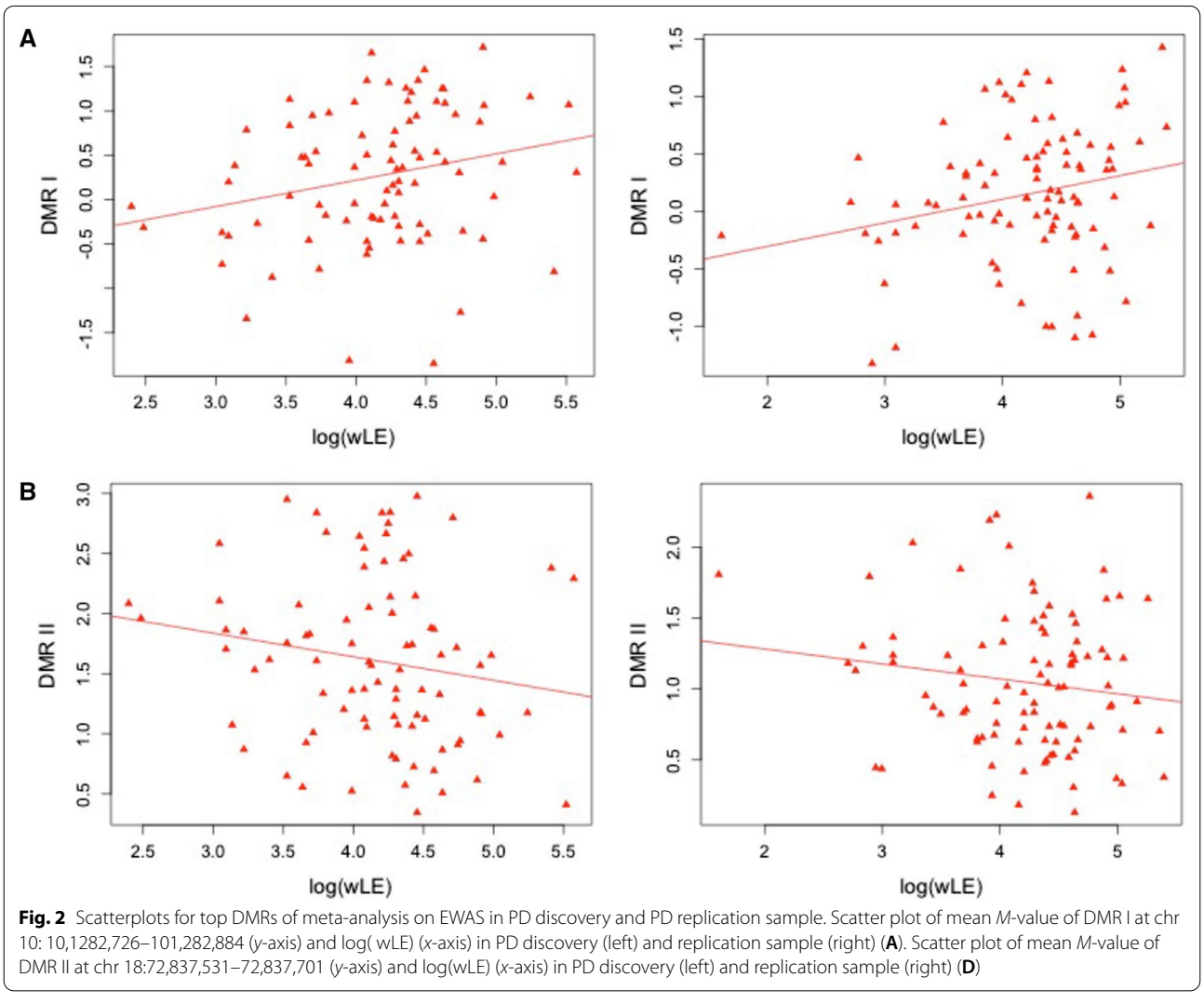

Fig. 2 Scatterplots for top DMRs of meta-analysis on EWAS in PD discovery and PD replication sample. Scatter plot of mean *M*-value of DMR I at chr 10: 10,1282,726–101,282,884 (*y*-axis) and log(wLE) (*x*-axis) in PD discovery (left) and replication sample (right) (**A**). Scatter plot of mean *M*-value of DMR II at chr 18:72,837,531–72,837,701 (*y*-axis) and log(wLE) (*x*-axis) in PD discovery (left) and replication sample (right) (**D**)

lower wLE, controls presented with higher DNAm levels with higher wLE.

EWAS on weighted stressful life events in major depressive disorder and meta-analysis with panic disorder

Finally, we assessed associations of wLE with DNAm levels in the MDD case sample (see Table 1) on an epigenome-wide scale (see Additional file 16: Fig. S15). We observed no associations surviving multiple testing correction. The top hit was cg00769012, an intronic CpG-site in *SYNGR1* on chromosome 22 ($p = 4.73 \times 10^{-05}$) where wLE was associated with higher DNAm levels. This CpG was not associated in the PD samples (p_meta = 0.31). As the MDD-sample presented with low power by itself, we meta-analyzed it with the PD discovery and replication sample (see Additional file 17: Fig. S16). The same two CpG-sites that had already evolved in the PD only analyses, presented also here with meta *p*-values $< 1.0 \times 10^{-05}$: cg03341655 in *GFOD2,* here the *p*-value got more significant when adding the MDD cases (p_meta $= 6.90 \times 10^{-06}$) indicating a replication (in MDD cases: beta = −0.0554, $p = 2.80 \times 10^{-01}$, also see Additional file 18: Fig. S17). For cg09738429, adding the MDD cases increased the *p*-value (p_meta $= 9.77 \times 10^{-06}$). To further evaluate if associations of wLE with DNAm were consistent in PD as well as in MDD cases, we investigated if direction of effects were different between PD cohorts and the MDD cohort. Focusing on the top-hits ($p < 1.0 \times 10^{-03}$) from the PD meta-analysis, we observed that only 53 out of 136 top CpG-sites available in all three cohorts presented with consistent effect across all three cohorts indicating that some top hits seem be specific to PD cases.

Discussion

The present study is the first to investigate the relationship of emotionally weighted life events on epigenome-wide DNAm in PD as diagnostic phenotype and its boundary to depression. No epigenome-wide significant results could be discerned in the PD cases meta-analysis; however, two CpG-sites presented with *p*-values below 1.0×10^{-05}: cg09738429 ($p = 6.40 \times 10^{-06}$, located in an intergenic shore region in the next proximity of *PYROXD1*) and cg03341655 ($p = = 8.14 \times 10^{-06}$, located in the exonic region of *GFOD2*). *PYROXD1* is involved in the response to oxidative stress [27]. Recent studies report higher DNAm in this gene in acute coronary syndrome and brain white matter lesions in older populations [28, 29]. Furthermore, a microarray-based post mortem analysis in human dorsal raphe nucleus tissue, a brain region pathophysiologically involved in serotonergic neurotransmission in MDD, showed a significant upregulation of the *PYROXD1* transcript in MDD cases vs. controls, corresponding to higher protein production related to MDD [30]. In our study, high wLE levels were associated with reduced DNAm suggesting higher gene expression, although we are not aware of any data evaluating the functional relevance of cg09738429 on gene regulation. Therefore, from this first results we can only speculate that high life time emotional stress could affect regulation of *PYROXD1* through DNAm. Additionally, positive EWAS associations at several CpG-sites in *PYROXD1* are available for adult smoking and maternal smoking in pregnancy [31–33]. Interestingly in relation to life stress, several investigations revealed also significant contributions of CpG-sites in *PYROXD1* as epigenetic markers for aging [34, 35].

Cg03341655, located in *GFOD2*, was the second top hit. Only for this CpG the significance level increased when patients with MDD were added to the meta-analysis suggesting a diagnosis independent effect of wLE on DNAm. *GFOD2* is highly expressed in the brain, predominantly in the cerebellum and cerebral cortex, lower expression has been shown in the hypothalamus and pituitary gland. However, its functional implication in psychiatric phenotypes, and specifically in anxiety, remains unclear. SNPs in the *GFOD2* have been associated with schizophrenia related phenotypes [36] and a recent study using a zebrafish model revealed its implication in the developing and adult brain as well as *GFOD2* expression in a subset of inhibitory GABA-neurons [37]. Variants in *GFOD2* have also been linked to the metabolic system and coronary disease, e.g., levels of circulating lipid levels and differential response to cholesterol-lowering diet [38]. One study showed negative correlation of DNAm of cg03341655 in the subcutaneous adipose tissue in response to high saturated fatty acids diet [39]. In fact, both, PD and MDD, as well as chronic stress are related to higher risk of metabolic syndromes and cardiovascular morbidity as has been shown in multiple studies [40–42]. Further EWAS have reported DNAm changes at different CpG-sites in *GFOD2* in relation to childhood abuse [43], maternal alcohol consumption and offspring cord blood methylation [44] and all-cause mortality in monozygotic twins [45]. These epigenetic studies suggest the relation of *GFOD2* DNAm status to a broad spectrum of stressful environmental conditions across life span.

One hypothesis for metabolic changes in anxiety and depression is the pronounced stimulation and putative hyperactivation of the endogenous stress system by life events [13, 46]. In MDD, this has also been related to higher age acceleration determined by epigenetic age markers [26]. However, no studies are available whether high levels of cortisol could lead to DNAm changes in *GFOD2*. One investigation in mice reports DNAm changes of the *Gfod2* gene in oocytes exposed to superovulation showing that gonadotropin hormones, at least

in a model with very high dosages, can induce DNAm changes in the respective gene [47]. However, the functional consequences of DNAm changes in *GFOD2* are widely unknown und further experiments involving neuroendocrine and metabolic measurements in reaction to stress are needed.

In summary, the analyses of differential DNAm in PD and MDD in response to wLE points to molecular targets implicated in the metabolic system, although the knowledge of the exact role of these first candidates remain limited. Nevertheless, pathway enrichment analysis primarily maps the top hits to genes expressed in the brain and secondly to blood vessels, suggesting that the present results map DNAm functionally involved in the transmission of stress effects also to brain systems.

The top hits from the analysis restricted to negative life events highly correlated with findings using the total life event composite score. When looking at positive life events, no previous EWAS data are available for our specific hits. However, EWAS have been published for other CpG-sites in the corresponding genes, presenting different directions of DNAm in association with disease phenotypes (e.g., for *TNXB* for maternal smoking and childhood abuse: [43, 48]). In the PD case–control interaction EWAS analysis on wLE, the best nominal association was located in the gene *NKAIN1,* showing opposite direction of DNAm in cases and controls with increasing values of wLE. *NKAIN1* is expressed in the brain, specifically in hippocampus, bus also in musculature and endocrine gland [49]. Variants in this gene have been associated with alcohol dependence [50] and autism spectrum disorder [51]. In the present study, only PD patients without history of alcohol dependence were included, suggesting that the differential DNAm methylation found here is not attributed to this phenotype. Indeed, the possible implication of *NKAIN1* in life stress related DNAm in PD as diagnosis remains unclear so far and further studies are needed to clarify how this gene is involved in the common and distinct biological pathways crossing PD, MDD and alcohol phenotypes.

We also conductd a DMR-analysis as this reveals more robust associations on regional clusters as compared to association analysis on single CpGs. The DMR analysis in PD patients resulted in two genomic regions significantly associated with differential methylation and wLE. The first DMR containing 4 CpGs (cg01987516, cg07044859, cg17888390 and cg23904955) is located on chr10 in an intergenic region between the genes *GOT1* and *DQ372722*. Higher DNAm of cg01987516 has been previously related to maternal anxiety in umbilical cord blood [52]. Furthermore, cg23904955 has been negatively correlated with ethanol consumption per day over the course of a year during the blood sample collection in a European population [53]. In addition, some CpGs have been positively correlated with insulin sensitivity and BMI in early childhood [54] and negatively corelated with smoking [31], which could be referred to the general field of metabolic health. The second significant DMR containing four CpGs on chromosome 18 is located in an intergenic region between the genes *ZNF407* and *ZADH2*. So far, no DNAm data on psychiatric phenotypes have been linked to this specific region. However, genetic variants as well as CpGs in both proximal genes have been associated with various phenotypes related to neuropsychiatric diseases. Genetic and methylation studies revealed associations in *ZNF407* with neurodevelopmental disorders, schizophrenia as well as Gulf War illness [55, 56]. One study points to the putative role of *ZNF407* in the regulation of insulin-stimulated glucose uptake [57]. Differential DNAm in *ZADH2* has been shown for suicidal attempts in schizophrenia [58], memory performance in Alzheimers disease [59], but also inflammatory phenotypes [60].

The present study offers the first results of DNAm in association with cumulative life events in PD and its boundary to depression. The interpretation of the results is limited by the moderate number of the included individuals. We study DNAm in blood and our results cannot be directly related to DNAm in brain. Investigations of tissue's average methylation for all CpGs between blood and brain show divergent correlation values, these values range from levels lower than 0.1 up to the overall blood–brain DNAm correlation of around 0.8 in a recent study [61]. Furthermore, PD patients were free of substance use disorders and were not medicated at the time of inclusion, but this does not account for putative psychiatric/non-psychiatric medication in the past. In contrast, MDD patients were medicated which could have influences on DNAm levels as has been shown by Barbu et al. [62]. Other factors not included in our analysis, such as childhood adversity, perinatal factors and further environmental influences might bias our analysis. Furthermore, the included PD cohorts cannot be treated as totally independent. The replication cohort is different in time of recruitment and time of DNAm measurement, however, similar in genetic architecture, assessment strategy and diagnostic evaluation given that both PD cohorts were recruited in the same center. It should also be noted that our study was performed on 450K arrays and hence, we could have missed potentially significant sites which are not covered on this array. Therefore, replication of our results in completely independent cohorts as well evaluation of CpGs covered by the EPIC array is necessary. However, by using a meta-analytic approach and adding MDD cases we aimed to provide a robust level of replication. Furthermore, we thoroughly corrected for

smoking, cell types, age as well as sex, which are important confounding variables.

Conclusions

In summary, this first DNAm analysis in PD reveal first evidence of small but significant DNAm changes in PD in association with cumulative stress-weighted life events. DMR analyses in PD rendered more disease-specific DNAm changes in relation to wLE in comparison to the EWAS, as seen by the additional analysis with MDD. Most of the top associated CpGs were located in genes implicated in metabolic processes supporting the hypothesis that environmental stress contributes to health damaging changes by affecting a broad spectrum of systems in the body which might contribute to age acceleration, as shown for affective disorders [26, 63]. The specificity of the DNAm results has to be replicated in independent samples providing measurement of endocrine, vascular and cardiac function in combination with DNAm and life stress in PD.

Methods

Study samples

Panic disorder (PD) discovery and replication sample

The PD discovery and replication sample are the same cohorts which were used in Iurato et al. [18] and were named as discovery and replication as they form two time-independent batches.

PD patients included in the discovery ($n=87$) and replication sample ($n=96$) were recruited in the anxiety disorders outpatient unit at the MPIP in Munich [21], (see Table 1 for demographic details). PD was the primary diagnosis ascertained by trained psychiatrists according to the Diagnostic and Statistical Manual of Mental Disorders (DSM)-IV criteria. Mild secondary depression was allowed. All patients underwent the Structured Clinical Interviews for DSM-IV (SCID I and II) [64]. PD due to a medical or neurological condition or the presence of a comorbid Axis II disorder was an exclusion criterion.

Control subjects were recruited from a Munich-based community sample and screened for the absence of axis I psychiatric disorders with the SCID [64]. Controls were age- and sex-matched with patients. To reduce confounding due to possible effects of drug treatment, both patients and controls were free of psychotropic medication for at least 4 weeks before the blood draw. All subjects were Caucasian and provided written informed consent. The Ethics Committee of the Ludwig Maximilians University, Munich, Germany, in accordance with the Declaration of Helsinki approved all procedures, Project number 318/00.

Major depressive disorder (MDD) sample

An independent sample of 102 depressed patients with information available on stressful life events was recruited at the MPIP. Recruitment strategies and detailed characterization of participants for the whole sample have been described elsewhere [65, 66]. In short, the diagnosis was ascertained by trained psychiatrists according to the DSM-IV criteria. Exclusion criteria were the presence of alcohol or substance abuse or dependence, comorbid somatization disorder, and depressive disorders owing to general medical or neurologic conditions. All patients were medicated. The study was approved by the local ethics committee and all individuals gave written informed consent.

Stressful life events (SLE)

Life events (LE) were assessed using the "Event List" [67], which is a German adaptation of the Social Readjustment Scale by Holmes et al. [68]. The event list includes 37 items assessing the occurrence and frequency (once, twice, several times) of typical life events including marriage, separation, change in life standards and habits, as well as death of close relatives and friends. Each item was additionally rated with respect to personal valency (very positive to very negative) and burden (not burdensome at all to extremely burdensome) on a 5-item Likert scale. From all 37 items a total life events score and a stress-weighted total life event score (wLE) were calculated reflecting the overall frequency of all life events and the overall life events frequency weighted by the individual burden score, respectively. In addition, items were categorized according to the individual valency score as positive or negative; the average number of positive life event items was 5.47 (ranging from 0 to 15), while the average number of negative life event items was 6.09 (ranging from 0 to 20). From these data, the numbers of positive and negative life events were calculated. In addition, weighted negative life events were obtained by weighting the reported event number with the individual burden scores (wnegLE), while weighted positive life events were derived by weighting the reported event number with the inverted individual burden scores (wposLE), reflecting positive life events weighted by individual relief.

To reduce the influence of extreme observations on the model parameters we applied a logarithmic transformation to wLE in the association analysis.

DNA methylation (DNAm) in PD sample

The pre-preprocessing is described in detail in [18]. Briefly, genomic DNA was extracted from peripheral blood and bisulfite converted DNA methylation levels were assessed for > 480,000 CpG sites using the Illumina

HumanMethylation450 BeadChip array. The Bioconductor R package *minfi* [69] was used for the quality control of DNAm data. Failed probes based on a detection *P*-value larger than 0.01 in > 50% of the samples as well and non-specific binding probes [70] and probes on X and Y chromosome were removed. We also excluded probes if single nucleotide polymorphisms (SNPs) were documented in the interval for which the Illumina probe is designed to hybridize. Probes located close (10 bp from query site) to a SNP which had a minor allele frequency of ≥ 0.05, as reported in the 1000 Genomes Project, were also removed. The data were then normalized with functional normalization [71]. Batch effects were identified using the Empirical Bayes' method *ComBat*. Batch corrected *M*-values after *ComBat* [72] were used for all further statistical analyses. Cell-type proportions were estimated from DNA methylation levels using the Houseman algorithm [73]. Furthermore, we derived smoking scores based on [74].

DNAm in MDD sample

Pre-processing is described in detail in [65]. Genomic DNA was extracted from whole blood and DNA methylation levels were assessed for > 480,000 CpG sites using the Illumina HumanMethylation450 BeadChip arrays. All methylation probes have been subjected to an extensive quality control including filtering by low p-detection value, functional normalization and batch correction with ComBat. Cellular composition was estimated by using CellCode [75]. Furthermore, we derived smoking scores based on Zeilinger et al. [74].

Statistical analyses

Epigenome-wide association analysis (EWAS) with wLE

First, within each cohort separately, association between log(wLE) and DNAm levels were assessed using linear regression models in R. The analysis was repeated on log(wposLE) and log(wnegLE). *M*-values of each CpG-site were used as dependent variable, log(wLE), log(wposLE) or log(wnegLE) respectively as independent variables. Age, sex, estimated cell type proportions as well as smoking score were used as covariates. For this analysis, only PD cases or MDD cases were included.

Case–control interaction with wLE

Within each PD cohort separately, we also tested for interaction between log(wLE), log(wposLE) and log (wnegLE) and PD case–control status on DNAm levels using linear regression models in R. *M*-values of each CpG-site were used as dependent variable, log(wLE) × PD case–control status as independent variable. The interaction model included the main effects of log(wLE) and PD case–control status. Age, sex, estimated cell type proportions as well as smoking score were used as covariates.

Meta-analysis

As PD discovery and replication were assessed timely independent of each other on the methylation arrays and hence can be considered as two independent batches, we meta-analysed the association results combining PD discovery and replication samples, a strategy which was also chosen in the original publication by Iurato et al. [18] who studied PD case–control effects on DNAm in these two cohorts. Meta-analysis combining PD discovery and replication samples as well as the MDD cohort (for the EWAS on wLE) was performed using PLINK v1.9. [76]. In PLINK, we used the meta-analysis command and report *p*-values from a fixed-effects meta-analysis. Overall, 424,763 CpGs were available in both PD cohorts and 308,360 CpGs across all three cohorts.

Manhattan- and QQ-plots

Manhattan- and QQ-plots were generated using the R-package *qqman.* Lambda-values were calculated using the R-package *QCEWAS.*

Differential methylation regions (DMRs)

In order to identify clusters of association results in the EWAS, we performed DMR analysis on the meta-analysis results from both PD samples based on the input of individual *p*-values of at least 5.0×10^{-05} and within 500 bp using comb-P [77].

Pathway enrichment

We used FUMA v1.3.6a [78], specifically the GENE2FUNC option, to test top hits for pathway enrichment. First, all CpG-site included in the PD meta-analysis were annotated to the nearest gene using the *matchGenes* function in the R-package *bumphunter* [79]. These 424,763 CpG-sites matched to 19,563 unique genes. This set was used as background. Next, we used all CpG-sites associated with a *p*-value < 0.01 in the meta-analysis of the PD case only analysis. These 1995 CpG-sites mapped to 1743 unique genes. This gene set was used as input set. These two genes sets were provided to the GENE2FUNC which runs Fisher-tests for enrichment of pathways, tissue specific genes in GTEx v8 [80] and genes identified in several GWAS. The FDR cut-off was set to 5% and a minimal overlap of 10 genes between gene-sets to be present.

Multiple testing correction

All association results were corrected for multiple testing at and false-discovery-rate (FDR) of 5% using the method of Benjamini and Hochberg [81].

Supplementary Information

The online version contains supplementary material available at https://doi.org/10.1186/s13148-022-01274-y.

Additional file 1: Figure S1. Overview of conducted analyses.

Additional file 2: Figure S2. Manhattan plot for EWAS of wLE in PDI cases. Chromosomal position is depicted on the *x*-axis, −log10(*p*-value) on the *y*-axis. The blue line indicates nominal *p*-values < 1.0×10^{-05} (A). QQ-plot for EWAS of wLE in PDI cases depicting expected −log10(*p*-values) versus observed −log10(*p*-values). The lambda-value is 0.83 (B).

Additional file 3: Figure S3. Manhattan plot for EWAS of wLE in PDII cases. Chromosomal position is depicted on the *x*-axis, −log10(*p*-value) on the *y*-axis. The blue line indicates nominal *p*-values< 1.0×10^{-05} (A). QQ-plot for EWAS of wLE in PDII cases depicting expected −log10(*p*-values) versus observed −log10(*p*-values). The lambda-value is 0.91 (B).

Additional file 4: Figure S4. Manhattan plot for meta-analysis of EWAS of wLE in PDI cases and PDII cases. Chromosomal position is depicted on the *x*-axis, −log10(*p*-value) on the *y*-axis. The blue line indicates nominal *p*-values < 1.0×10^{-05} (A). QQ-plot for meta-analysis of EWAS of wLE in PDI cases and PDII cases depicting expected −log10(*p*-values) versus observed −log10(*p*-values). The lambda-value is 0.86 (B).

Additional file 5: Figure S5. Manhattan plot for EWAS of wposLE in PDI cases. Chromosomal position is depicted on the *x*-axis, −log10(*p*-value) on the *y*-axis. The blue line indicates nominal *p*-values < 1.0×10^{-05} (A). QQ-plot for EWAS of wposLE in PDI cases depicting expected −log10(*p*-values) versus observed −log10(*p*-values). The lambda-value is 0.92 (B).

Additional file 6: Figure S6. Manhattan plot for EWAS of wposLE in PDII cases. Chromosomal position is depicted on the *x*-axis, −log10(*p*-value) on the *y*-axis. The blue line indicates nominal *p*-values < 1.0×10^{-05} (A). QQ-plot for EWAS of wposLE in PDII cases depicting expected −log10(*p*-values) versus observed −log10(*p*-values). The lambda-value is 1.00 (B).

Additional file 7: Figure S7. Manhattan plot for meta-analysis of EWAS of wposLE in PDI cases and PDII cases. Chromosomal position is depicted on the *x*-axis, −log10(*p*-value) on the *y*-axis. The blue line indicates nominal *p*-values < 1.0×10^{-05} (A). QQ-plot for meta-analysis of EWAS of wposLE in PDI cases and PDII cases depicting expected −log10(*p*-values) versus observed −log10(*p*-values). The lambda-value is 1.00 (B).

Additional file 8: Figure S8. Manhattan plot for EWAS of wnegLE in PDI cases. Chromosomal position is depicted on the *x*-axis, −log10(*p*-value) on the *y*-axis. The blue line indicates nominal *p*-values < 1.0×10^{-05} (A). QQ-plot for EWAS of wnegLE in PDI cases depicting expected −log10(*p*-values) versus observed −log10(*p*-values). The lambda-value is 0.91 (B).

Additional file 9: Figure S9. Manhattan plot for EWAS of wnegLE in PDII cases. Chromosomal position is depicted on the *x*-axis, −log10(*p*-value) on the *y*-axis. The blue line indicates nominal *p*-values < 1.0×10^{-05} (**A**). QQ-plot for EWAS of wnegLE in PDII cases depicting expected −log10(*p*-values) versus observed −log10(*p*-values). The lambda-value is 0.94 (**B**).

Additional file 10: Figure S10. Manhattan plot for meta-analysis of EWAS of wnegLE in PDI cases and PDII cases. Chromosomal position is depicted on the *x*-axis, −log10(*p*-value) on the *y*-axis. The blue line indicates nominal *p*-values < 1.0×10^{-05} (A). QQ-plot for meta-analysis of EWAS of wnegLE in PDI cases and PDII cases depicting expected −log10(*p*-values) versus observed −log10(*p*-values). The lambda-value is 0.95 (B).

Additional file 11: Table S1. CpGs associated with weighted positive life-events in the meta-analysis of PD discovery and replication cases at $p < 1.0 \times 10^{-05}$. **Table S2**. CpGs associated with weighted negative life-events in the meta-analysis of PD discovery and replication cases at $p < 1.0 \times 10^{-05}$. **Table S3**. Enrichment analysis of top-hits in the meta-analysis of weighted life events of PD discovery and replication cases with regards to tissue specificity in GTEx. **Table S4**. Enrichment analysis of hypermethylated top-hits in the meta-analysis of weighted life events of PD discovery and replication cases with regards to tissue specificity in GTEx. **Table S5**. Enrichment analysis of hypomethylated top-hits in the meta-analysis of weighted life events of PD discovery and replication cases with regards to tissue specificity in GTEx. **Table S6**. Enrichment analysis of top-hits in the meta-analysis of weighted life events in PD discovery and replication caess with regards to GO biological processes. **Table S7**. Enrichment analysis of hypermethylated top-hits in the meta-analysis of weighted life events in PD discovery and replication caess with regards to GO biological processes. **Table S8**. Enrichment analysis of hypomethylated top-hits in the meta-analysis of weighted life events of PD discovery and replication cases with regards to tissue specificity. **Table S9**. CpGs associated with weighted life-events x case-control status in the meta-analysis of PD discovery and replication sample at $p < 1.0 \times 10^{-05}$.

Additional file 12: Figure S11. Manhattan plot for EWAS of wLE x case-control-status in PDI. Chromosomal position is depicted on the *x*-axis, −log10(*p*-value) on the *y*-axis. The blue line indicates nominal *p*-values <1.0×10^{-05} (A). QQ-plot for EWAS of wLE x case-control-status in PDI depicting expected −log10(*p*-values) versus observed −log10(*p*-values). The lambda-value is 1.02 (B).

Additional file 13: Figure S12. Manhattan plot for EWAS of wLE x case-control-status in PDII. Chromosomal position is depicted on the *x*-axis, −log10(*p*-value) on the *y*-axis. The blue line indicates nominal *p*-values < 1.0×10^{-05} (A). QQ-plot for EWAS of wLE x case-control-status in PDII depicting expected −log10(*p*-values) versus observed −log10(*p*-values). The lambda-value is 0.99 (B).

Additional file 14: Figure S13. Manhattan plot for meta-analysis of EWAS of wLE x case-control-status in PDI and PDII. Chromosomal position is depicted on the *x*-axis, −log10(*p*-value) on the *y*-axis. The blue line indicates nominal *p*-values < 1.0×10^{-05} (A). QQ-plot for meta-analysis of EWAS of of wLE x case-control-status in PDI and PDII depicting expected −log10(*p*-values) versus observed −log10(*p*-values). The lambda-value is 1.02 (B).

Additional file 15: Figure S14. Scatterplots in PDI (above) and PDII (below) forF wigLuE on DNAm of cg20941758. The *x*-axis denotes log(wLE), the *y*-axis denotes *M*-value of cg20941758, PD cases are depicted in red, controls in green. The red line indicates the regression line in PD cases, the green line in controls.

Additional file 16: Figure S15. Manhattan plot for EWAS of wLE in MDD cases. Chromosomal position is depicted on the *x*-axis, −log10(*p*-value) on the *y*-axis. The blue line indicates nominal *p*-values < 1.0×10^{-05} (A). QQ-plot for EWAS of wLE in MDD cases depicting expected −log10(*p*-values) versus observed −log10(*p*-values). The lambda-value is 0.79 (B).

Additional file 17: Figure S16. Manhattan plot for meta-analysis of EWAS of wLE in PDI cases, PDII cases and MDD cases. Chromosomal position is depicted on the *x*-axis, −log10(*p*-value) on the *y*-axis. The blue line indicates nominal *p*-values <1.0×10^{-05} (A). QQ-plot for meta-analysis of EWAS of wLE in PDI cases, PDII cases and MDD cases cases depicting expected −log10(*p*-values) versus observed −log10(*p*-values). The lambda-value is 0.85 (B).

Additional file 18: Figure S17. Scatterplots in PD discovery (above), PD replication (middle) and MDD sample (below) for wLE on DNAm of cg03341655. The *x*-axis denotes log(wLE), the *y*-axis denotes *M*-value of cg03341655. The black line indicates the regression line.

Acknowledgments

We thank all study participants who enabled the present analysis and the MPI Biobank staff for support in the processing of biosamples.

Author contributions

DC analyzed and interpreted the data, prepared and edited tables and figures and wrote and edited the manuscript. AN and RD analyzed the data. SI, JA and JM were involved in the pre-processing of the data. MI, EB and AE interpreted the data and edited the manuscript. All authors read and approved the final manuscript.

Funding

Open Access funding enabled and organized by Projekt DEAL. The study was supported by the Eranet Neuron AnxBio (01EW1401A).

Availability of data and materials
DNA methylation levels as well PD and weighted life events scores for PDI and PDII have been deposited in NCBI's Gene Expression Omnibus and are accessible through GEO Series accession number GSE201016 (https://www.ncbi.nlm.nih.gov/geo/query/acc.cgi?acc=GSE201016).

Declarations

Ethics approval and consent to participate
The Ethics Committee of the Ludwig Maximilians University, Munich, Germany, in accordance with the Declaration of Helsinki approved all procedures.

Consent for publication
Not applicable.

Competing interests
EB is the coinventor of FKBP5: a novel target for antidepressant therapy, European Patent no. EP 1687443 B1, and receives a research grant from Böhringer Ingelheim for a collaboration on functional investigations of FKBP5. It has to be noted that SI is now a full-time employee at Roche Diagnostics GmbH and JM is a full-time employee at Capgemini Deutschland GmbH. Otherwise, the authors declare that they have no competing interests.

Author details
[1]Translational Department, Max Planck Institute for Psychiatry, Kraepelinstrasse 2+10, 80804 Munich, Germany. [2]Institute of Statistics, Faculty of Mathematics, Informatics and Statistics, Ludwig-Maximilians-University Munich, Munich, Germany. [3]Department of Psychiatry and Behavioral Sciences, School of Medicine, Emory University, Atlanta, GA, USA. [4]Department of Psychiatry, Psychosomatics and Psychotherapy, Centre of Mental Health, Julius-Maximilians-University, Wuerzburg, Germany.

Received: 21 January 2022 Accepted: 7 April 2022
Published online: 27 April 2022

References

1. APA. Diagnostic and statstical manual of mental disorders (DMS-V), 2013.
2. Baxter AJ, Vos T, Scott KM, Ferrari AJ, Whiteford HA. The global burden of anxiety disorders in 2010. Psychol Med. 2014;44(11):2363–74.
3. Goodwin RD, Faravelli C, Rosi S, Cosci F, Truglia E, de Graaf R, et al. The epidemiology of panic disorder and agoraphobia in Europe. Eur Neuropsychopharmacol. 2005;15(4):435–43.
4. Jacobi F, Hofler M, Siegert J, Mack S, Gerschler A, Scholl L, et al. Twelve-month prevalence, comorbidity and correlates of mental disorders in Germany: the Mental Health Module of the German Health Interview and Examination Survey for Adults (DEGS1-MH). Int J Methods Psychiatr Res. 2014;23(3):304–19.
5. Kessler RC, Avenevoli S, Costello J, Green JG, Gruber MJ, McLaughlin KA, et al. Severity of 12-month DSM-IV disorders in the National Comorbidity Survey Replication Adolescent Supplement. Arch Gen Psychiatry. 2012;69(4):381–9.
6. Kessler RC, Stang PE, Wittchen HU, Ustun TB, Roy-Burne PP, Walters EE. Lifetime panic-depression comorbidity in the National Comorbidity Survey. Arch Gen Psychiatry. 1998;55(9):801–8.
7. Chen MH, Tsai SJ. Treatment-resistant panic disorder: clinical significance, concept and management. Prog Neuropsychopharmacol Biol Psychiatry. 2016;70:219–26.
8. Meier SM, Trontti K, Purves KL, Als TD, Grove J, Laine M, et al. Genetic variants associated with anxiety and stress-related disorders: a genome-wide association study and mouse-model study. JAMA Psychiat. 2019;76(9):924–32.
9. Ask H, Cheesman R, Jami ES, Levey DF, Purves KL, Weber H. Genetic contributions to anxiety disorders: where we are and where we are heading. Psychol Med. 2021;51(13):2231–46.
10. Hettema JM, Prescott CA, Myers JM, Neale MC, Kendler KS. The structure of genetic and environmental risk factors for anxiety disorders in men and women. Arch Gen Psychiatry. 2005;62(2):182–9.
11. Nugent NR, Tyrka AR, Carpenter LL, Price LH. Gene-environment interactions: early life stress and risk for depressive and anxiety disorders. Psychopharmacology. 2011;214(1):175–96.
12. Asselmann E, Stender J, Grabe HJ, Konig J, Schmidt CO, Hamm AO, et al. Assessing the interplay of childhood adversities with more recent stressful life events and conditions in predicting panic pathology among adults from the general population. J Affect Disord. 2018;225:715–22.
13. Dirven BCJ, Homberg JR, Kozicz T, Henckens M. Epigenetic programming of the neuroendocrine stress response by adult life stress. J Mol Endocrinol. 2017;59(1):R11–31.
14. Lin E, Tsai S-J. Gene-environment interactions and role of epigenetics in anxiety disorders. In: Kim Y-K, editor. Anxiety disorders: rethinking and understanding recent discoveries. Singapore: Springer; 2020. p. 93–102.
15. Klengel T, Pape J, Binder EB, Mehta D. The role of DNA methylation in stress-related psychiatric disorders. Neuropharmacology. 2014;80:115–32.
16. Schiele MA, Domschke K. Epigenetics at the crossroads between genes, environment and resilience in anxiety disorders. Genes Brain Behav. 2018;17(3):e12423.
17. Emeny RT, Baumert J, Zannas AS, Kunze S, Wahl S, Iurato S, et al. Anxiety associated increased CpG methylation in the promoter of Asb1: a translational approach evidenced by epidemiological and clinical studies and a murine model. Neuropsychopharmacology. 2018;43(2):342–53.
18. Iurato S, Carrillo-Roa T, Arloth J, Czamara D, Diener-Holzl L, Lange J, et al. "DNA Methylation signatures in panic disorder. Transl Psychiatry. 2017;7(12):1287.
19. Domschke K, Tidow N, Schrempf M, Schwarte K, Klauke B, Reif A, et al. Epigenetic signature of panic disorder: a role of glutamate decarboxylase 1 (GAD1) DNA hypomethylation? Prog Neuropsychopharmacol Biol Psychiatry. 2013;46:189–96.
20. Domschke K, Tidow N, Kuithan H, Schwarte K, Klauke B, Ambree O, et al. Monoamine oxidase A gene DNA hypomethylation: a risk factor for panic disorder? Int J Neuropsychopharmacol. 2012;15(9):1217–28.
21. Erhardt A, Czibere L, Roeske D, Lucae S, Unschuld PG, Ripke S, et al. TMEM132D, a new candidate for anxiety phenotypes: evidence from human and mouse studies. Mol Psychiatry. 2011;16(6):647–63.
22. Naik RR, Sotnikov SV, Diepold RP, Iurato S, Markt PO, Bultmann A, et al. Polymorphism in Tmem132d regulates expression and anxiety-related behavior through binding of RNA polymerase II complex. Transl Psychiatry. 2018;8(1):1.
23. Kessler RC, Chiu WT, Jin R, Ruscio AM, Shear K, Walters EE. The epidemiology of panic attacks, panic disorder, and agoraphobia in the National Comorbidity Survey Replication. Arch Gen Psychiatry. 2006;63(4):415–24.
24. Roy-Byrne PP, Stang P, Wittchen HU, Ustun B, Walters EE, Kessler RC. Lifetime panic-depression comorbidity in the National Comorbidity Survey. Association with symptoms, impairment, course and help-seeking. Br J Psychiatry. 2000;176:229–35.
25. Brainstorm C, Anttila V, Bulik-Sullivan B, Finucane HK, Walters RK, Bras J, et al. Analysis of shared heritability in common disorders of the brain. Science. 2018;360(6395):eaap8757.
26. Zannas AS, Arloth J, Carrillo-Roa T, Iurato S, Roh S, Ressler KJ, et al. Lifetime stress accelerates epigenetic aging in an urban, African American cohort: relevance of glucocorticoid signaling. Genome Biol. 2015;16:266.
27. Asanovic I, Strandback E, Kroupova A, Pasajlic D, Meinhart A, Tsung-Pin P, et al. The oxidoreductase PYROXD1 uses NAD(P)(+) as an antioxidant to sustain tRNA ligase activity in pre-tRNA splicing and unfolded protein response. Mol Cell. 2021;81(12):2520–32.
28. Huang WQ, Yi KH, Li Z, Wang H, Li ML, Cai LL, et al. DNA methylation profiling reveals the change of inflammation-associated ZC3H12D in leukoaraiosis. Front Aging Neurosci. 2018;10:143.
29. Li D, Yan J, Yuan Y, Wang C, Wu J, Chen Q, et al. Genome-wide DNA methylome alterations in acute coronary syndrome. Int J Mol Med. 2018;41(1):220–32.
30. Kerman IA, Bernard R, Bunney WE, Jones EG, Schatzberg AF, Myers RM, et al. Evidence for transcriptional factor dysregulation in the dorsal raphe nucleus of patients with major depressive disorder. Front Neurosci. 2012;6:135.
31. Joehanes R, Just AC, Marioni RE, Pilling LC, Reynolds LM, Mandaviya PR, et al. Epigenetic signatures of cigarette smoking. Circ Cardiovasc Genet. 2016;9(5):436–47.

32. Joubert BR, Felix JF, Yousefi P, Bakulski KM, Just AC, Breton C, et al. DNA methylation in newborns and maternal smoking in pregnancy: genome-wide consortium meta-analysis. Am J Hum Genet. 2016;98(4):680–96.
33. O'Grady GL, Best HA, Sztal TE, Schartner V, Sanjuan-Vazquez M, Donkervoort S, et al. Variants in the oxidoreductase PYROXD1 cause early-onset myopathy with internalized nuclei and myofibrillar disorganization. Am J Hum Genet. 2016;99(5):1086–105.
34. Li C, Gao W, Gao Y, Yu C, Lv J, Lv R, et al. Age prediction of children and adolescents aged 6–17 years: an epigenome-wide analysis of DNA methylation. Aging (Albany NY). 2018;10(5):1015–26.
35. Yusipov I, Bacalini MG, Kalyakulina A, Krivonosov M, Pirazzini C, Gensous N, et al. Age-related DNA methylation changes are sex-specific: a comprehensive assessment. Aging (Albany NY). 2020;12(23):24057–80.
36. Gusev A, Mancuso N, Won H, Kousi M, Finucane HK, Reshef Y, et al. Transcriptome-wide association study of schizophrenia and chromatin activity yields mechanistic disease insights. Nat Genet. 2018;50(4):538–48.
37. Lechermeier CG, D'Orazio A, Romanos M, Lillesaar C, Drepper C. Distribution of transcripts of the GFOD gene family members gfod1 and gfod2 in the zebrafish central nervous system. Gene Expr Patterns. 2020;36:119111.
38. Guevara-Cruz M, Lai CQ, Richardson K, Parnell LD, Lee YC, Tovar AR, et al. Effect of a GFOD2 variant on responses in total and LDL cholesterol in Mexican subjects with hypercholesterolemia after soy protein and soluble fiber supplementation. Gene. 2013;532(2):211–5.
39. Perfilyev A, Dahlman I, Gillberg L, Rosqvist F, Iggman D, Volkov P, et al. Impact of polyunsaturated and saturated fat overfeeding on the DNA-methylation pattern in human adipose tissue: a randomized controlled trial. Am J Clin Nutr. 2017;105(4):991–1000.
40. Batelaan NM, Seldenrijk A, Bot M, van Balkom AJ, Penninx BW. Anxiety and new onset of cardiovascular disease: critical review and meta-analysis. Br J Psychiatry. 2016;208(3):223–31.
41. Lindekilde N, Rutters F, Erik Henriksen J, Lasgaard M, Schram MT, Rubin KH, et al. Psychiatric disorders as risk factors for type 2 diabetes: an umbrella review of systematic reviews with and without meta-analyses. Diabetes Res Clin Pract. 2021;176:108855.
42. Shea S, Lionis C, Kite C, Atkinson L, Chaggar SS, Randeva HS, et al. Non-alcoholic fatty liver disease (NAFLD) and potential links to depression, anxiety, and chronic stress. Biomedicines. 2021;9(11):1697.
43. Yang BZ, Zhang H, Ge W, Weder N, Douglas-Palumberi H, Perepletchikova F, et al. Child abuse and epigenetic mechanisms of disease risk. Am J Prev Med. 2013;44(2):101–7.
44. Sharp GC, Arathimos R, Reese SE, Page CM, Felix J, Kupers LK, et al. Maternal alcohol consumption and offspring DNA methylation: findings from six general population-based birth cohorts. Epigenomics. 2018;10(1):27–42.
45. Svane AM, Soerensen M, Lund J, Tan Q, Jylhava J, Wang Y, et al. DNA methylation and all-cause mortality in middle-aged and elderly danish twins. Genes (Basel). 2018;9(2):78.
46. Vinkers CH, Kuzminskaite E, Lamers F, Giltay EJ, Penninx B. An integrated approach to understand biological stress system dysregulation across depressive and anxiety disorders. J Affect Disord. 2021;283:139–46.
47. Huo Y, Yan ZQ, Yuan P, Qin M, Kuo Y, Li R, et al. Single-cell DNA methylation sequencing reveals epigenetic alterations in mouse oocytes superovulated with different dosages of gonadotropins. Clin Epigenetics. 2020;12(1):75.
48. Miyake K, Kawaguchi A, Miura R, Kobayashi S, Tran NQV, Kobayashi S, et al. Association between DNA methylation in cord blood and maternal smoking: The Hokkaido Study on Environment and Children's Health. Sci Rep. 2018;8(1):5654.
49. Gorokhova S, Bibert S, Geering K, Heintz N. A novel family of transmembrane proteins interacting with beta subunits of the Na, K-ATPase. Hum Mol Genet. 2007;16(20):2394–410.
50. Zuo L, Wang K, Zhang XY, Krystal JH, Li CS, Zhang F, et al. NKAIN1-SERINC2 is a functional, replicable and genome-wide significant risk gene region specific for alcohol dependence in subjects of European descent. Drug Alcohol Depend. 2013;129(3):254–64.
51. Hnoonual A, Thammachote W, Tim-Aroon T, Rojnueangnit K, Hansakunachai T, Sombuntham T, et al. Chromosomal microarray analysis in a cohort of underrepresented population identifies SERINC2 as a novel candidate gene for autism spectrum disorder. Sci Rep. 2017;7(1):12096.
52. Sammallahti S, Cortes Hidalgo AP, Tuominen S, Malmberg A, Mulder RH, Brunst KJ, et al. Maternal anxiety during pregnancy and newborn epigenome-wide DNA methylation. Mol Psychiatry. 2021;26(6):1832–45.
53. Liu C, Marioni RE, Hedman AK, Pfeiffer L, Tsai PC, Reynolds LM, et al. A DNA methylation biomarker of alcohol consumption. Mol Psychiatry. 2018;23(2):422–33.
54. van Dijk SJ, Peters TJ, Buckley M, Zhou J, Jones PA, Gibson RA, et al. DNA methylation in blood from neonatal screening cards and the association with BMI and insulin sensitivity in early childhood. Int J Obes (Lond). 2018;42(1):28–35.
55. Jaffe AE, Gao Y, Deep-Soboslay A, Tao R, Hyde TM, Weinberger DR, et al. Mapping DNA methylation across development, genotype and schizophrenia in the human frontal cortex. Nat Neurosci. 2016;19(1):40–7.
56. Trivedi MS, Abreu MM, Sarria L, Rose N, Ahmed N, Beljanski V, et al. Alterations in DNA methylation status associated with Gulf war illness. DNA Cell Biol. 2019;38(6):561–71.
57. Buchner DA, Charrier A, Srinivasan E, Wang L, Paulsen MT, Ljungman M, et al. Zinc finger protein 407 (ZFP407) regulates insulin-stimulated glucose uptake and glucose transporter 4 (Glut4) mRNA. J Biol Chem. 2015;290(10):6376–86.
58. Bani-Fatemi A, Adanty C, Dai N, Dada O, Strauss J, Zai C, et al. Genome-wide methylation association with current suicidal ideation in schizophrenia. J Neural Transm (Vienna). 2020;127(9):1315–22.
59. Madrid A, Hogan KJ, Papale LA, Clark LR, Asthana S, Johnson SC, et al. DNA hypomethylation in blood links B3GALT4 and ZADH2 to Alzheimer's disease. J Alzheimers Dis. 2018;66(3):927–34.
60. Yeung EH, Guan W, Zeng X, Salas LA, Mumford SL, de Prado BP, et al. Cord blood DNA methylation reflects cord blood C-reactive protein levels but not maternal levels: a longitudinal study and meta-analysis. Clin Epigenetics. 2020;12(1):60.
61. Braun PR, Han S, Hing B, Nagahama Y, Gaul LN, Heinzman JT, et al. Genome-wide DNA methylation comparison between live human brain and peripheral tissues within individuals. Transl Psychiatry. 2019;9(1):47.
62. Barbu MC, Huider F, Campbell A, Amador C, Adams MJ, Lynall ME, et al. Methylome-wide association study of antidepressant use in Generation Scotland and the Netherlands Twin Register implicates the innate immune system. Mol Psychiatry. 2021. https://doi.org/10.1038/s41380-021-01412-7.
63. Dammering F, Martins J, Dittrich K, Czamara D, Rex-Haffner M, Overfeld J, et al. The pediatric buccal epigenetic clock identifies significant ageing acceleration in children with internalizing disorder and maltreatment exposure. Neurobiol Stress. 2021;15:100394.
64. Wittchen HU, Zaudig M, Fydrich T. SKID Strukturiertes Klinisches Interview für DSM-IV. Z Klin Psychol Psychother. 1999;28:68–70.
65. Arloth J, Bogdan R, Weber P, Frishman G, Menke A, Wagner KV, et al. Genetic differences in the immediate transcriptome response to stress predict risk-related brain function and psychiatric disorders. Neuron. 2015;86(5):1189–202.
66. Menke A, Arloth J, Putz B, Weber P, Klengel T, Mehta D, et al. Dexamethasone stimulated gene expression in peripheral blood is a sensitive marker for glucocorticoid receptor resistance in depressed patients. Neuropsychopharmacology. 2012;37(6):1455–64.
67. Ising M, Lauer CJ, Holsboer F, Modell S. Münchner Vulnerabilitätsstudie: Beitrag von High Risk-Studien zur Verlaufsforschung. In: Sokya M, H.-J. M, Wittchen HU, editors. Psychopathologie im Längsschnitt. Landsberg: Ecomed; 2003. p. 148–60.
68. Holmes TH, Rahe RH. The social readjustment rating scale. J Psychosom Res. 1967;11(2):213–8.
69. Aryee MJ, Jaffe AE, Corrada-Bravo H, Ladd-Acosta C, Feinberg AP, Hansen KD, et al. Minfi: a flexible and comprehensive Bioconductor package for the analysis of Infinium DNA methylation microarrays. Bioinformatics. 2014;30(10):1363–9.
70. Chen YA, Lemire M, Choufani S, Butcher DT, Grafodatskaya D, Zanke BW, et al. Discovery of cross-reactive probes and polymorphic CpGs in the Illumina Infinium HumanMethylation450 microarray. Epigenetics. 2013;8(2):203–9.
71. Fortin JP, Labbe A, Lemire M, Zanke BW, Hudson TJ, Fertig EJ, et al. Functional normalization of 450k methylation array data improves replication in large cancer studies. Genome Biol. 2014;15(12):503.

72. Johnson WE, Li C, Rabinovic A. Adjusting batch effects in microarray expression data using empirical Bayes methods. Biostatistics. 2007;8(1):118–27.
73. Houseman EA, Accomando WP, Koestler DC, Christensen BC, Marsit CJ, Nelson HH, et al. DNA methylation arrays as surrogate measures of cell mixture distribution. BMC Bioinform. 2012;13:86.
74. Zeilinger S, Kuhnel B, Klopp N, Baurecht H, Kleinschmidt A, Gieger C, et al. Tobacco smoking leads to extensive genome-wide changes in DNA methylation. PLoS ONE. 2013;8(5):e63812.
75. Chikina M, Zaslavsky E, Sealfon SC. CellCODE: a robust latent variable approach to differential expression analysis for heterogeneous cell populations. Bioinformatics. 2015;31(10):1584–91.
76. Purcell S, Neale B, Todd-Brown K, Thomas L, Ferreira MA, Bender D, et al. PLINK: a tool set for whole-genome association and population-based linkage analyses. Am J Hum Genet. 2007;81(3):559–75.
77. Pedersen BS, Schwartz DA, Yang IV, Kechris KJ. Comb-p: software for combining, analyzing, grouping and correcting spatially correlated P-values. Bioinformatics. 2012;28(22):2986–8.
78. Watanabe K, Taskesen E, van Bochoven A, Posthuma D. Functional mapping and annotation of genetic associations with FUMA. Nat Commun. 2017;8(1):1826.
79. Jaffe AE, Murakami P, Lee H, Leek JT, Fallin MD, Feinberg AP, et al. Bump hunting to identify differentially methylated regions in epigenetic epidemiology studies. Int J Epidemiol. 2012;41(1):200–9.
80. Consortium GT. The Genotype-Tissue Expression (GTEx) project. Nat Genet. 2013;45(6):580–5.
81. Benjamini Y, Drai D, Elmer G, Kafkafi N, Golani I. Controlling the false discovery rate in behavior genetics research. Behav Brain Res. 2001;125(1–2):279–84.

Publisher's Note